GRAVITY ANOMALY AND GRADIENT RECOVERY FROM GOCE GRADIENT DATA USING LSC AND COMPARISONS WITH KNOWN GROUND DATA

C.C. Tscherning[1] and D.N. Arabelos[2]

[1]*Niels Bohr Institute, University of Copenhagen, Juliane Maries vej 32, DK-2100, Copenhagen Oe, Denmark*
[2]*Department of Geodesy and Surveying, Aristotle University of Thessaloniki, GR-54124, Thessaloniki, Greece*

ABSTRACT

The recovery of the free air gravity anomaly and the vertical gravity gradient in places of the Earth with known ground data is done using Least-Squares Collocation (LSC) with real GOCE TRF gradient data covering a period of two years. *Tzz* and *Txx* components are used separately or in combination as input data. The use of *Tzz* yields generally better results than *Txx*, while the combination of both improves marginally the results yielded by *Tzz* only. The computations show that both, distribution of input data and their adopted accuracy affect the prediction results. The best results are in areas with a smooth gravity fields, where the difference between computed and point values is of the order of 12 mGal. We furthermore compare the results of the prediction using collocation with corresponding results of the computation of the gravity anomalies using the GOCE models SPW, TIM and DIR, release 1 and the TIM, DIR, release 2.

Key words: least squares collocation; GOCE TRF gradients; GOCE EGMs

1. INTRODUCTION

Simulation investigations have been carried out many years ago before GOCE data become available, in the frame of numerous projects supported by ESA. Recently, with the release of the real GOCE data we have the opportunity to discover how close to the reality were our simulation studies. The data are gravity gradients of the Earth potential, *V*. In the pollowing we work with anomalous quantities, i.e. gradients applied on $T=V-U$, where U is the GRS80 normal potential without the centrifugal term.

Prediction experiments for the recovery of gravity anomalies from GOCE data using Least Squares Collocation (LSC) were carried out in order to investigate the information included in *Tzz* or/and *Txx* beyond degree 36 of the gravity spectrum. The contribution of EGM96 (Lemoine et. Al, 1998) from degree 2 to 36 were subtracted (and later restored) in order to permit the use of spherical approximation in LSC. The GRAVSOFT (Forsberg and Tscherning, 2008) program GEOCOL (Tscherning, 1974) was used for this purpose.

The recently available GOCE data *Tzz* and *Txx* were used for the prediction of gravity anomalies in different areas of the Earth, where gravity data have been recently used for the assessment of the Earth gravitational models (EGM)s EGM96, EIGENGL04C and EGM2008 (see, Arabelos and Tscherning, 2010). (The z-axis is in the direction of the radius-vector and the x-axis points North).These areas, presenting different characteristics of the gravity field are located in the Arctic zone, in Antarctica, in the Canadian plains, in Scandinavia, in Oklahoma, in the Mediterranean Sea, in Taiwan, and in Australia. Simultaneously, several parameters affecting the prediction quality were investigated such as the

- effect of the combination of *Tzz* with *Txx*,
- error hypothesis of input data,
- distribution and density of the input data,
- sensitivity of the results on the estimated covariance function,
- variability of the gravity field.

The results of the prediction are compared with the results of the reduction of the same test gravity observations to the recently released GOCE EGMs SPW, TIM and DIR release 1 and TIM and DIR, release 2, which are then referred to as TIM2 and DIR2. The comparison showed discrepancies between the results of the prediction and the reduction. Results are below shown for the release 1 and 2 models The two release 2 models show very small differences with respect to release 1.

To resolve the problem, the available GOCE gradient *Tzz* and *Txx* data given in the terrestrial reference frame (see HPF, 2010) are compared with corresponding data generated from the EGMs. In Oklahoma for instance the difference in terms of the standard deviation between the GOCE *Tzz* observations and the *Tzz* generated from DIR equals to 0.013343 EU. This means that there is a signal

included in DIR which is not included in *Tzz* data, or that there is a noise included in the *Tzz* data that is filtered in DIR.

To investigate further the problem, experiments of gravity prediction were carried out using *Tzz* data generated from DIR. The results of these experiments in terms of the standard deviation of the differences between observed and predicted gravity data are in significantly better agreement with corresponding results of the reduction of the same test data to DIR, than those where GOCE data were used for the prediction.

The not negligible differences of the reduction results among the three GOCE models are obviously due to different degree of expansion and to particular features of each model.

An attempt to recover *Tzz* gradients at GOCE orbit altitude from surface gravity anomalies over Taiwan showed poor quality results compared to *Tzz* gradients generated from the EGMs.

Finally, the prediction of GGSS *Tzz* over Oklahoma from GOCE *Tzz* observation, as well as the reduction of GGSS (Gravity Gradiometer Survey System) *Tzz* to the GOCE EGMs was extremely unsuccessful.

2. Computations

The test areas where gravity data are available in this investigation are of different extent, the data are point or mean free air gravity anomalies and the density of the data varies from one area to another. More details about the test data are included in (Arabelos and Tscherning, 2010).

On the other hand the density of the available GOCE gradient data depends on the latitude, with much fewer data distributed at low latitudes.

Due to these reasons, in our experiments we have used all the available GOCE data in Oklahoma, Taiwan and in the Mediterranean Sea, while in areas of higher latitude such as the Canadian plains, Scandinavia, Australia, Arctic zone, and Antarctica, a thinner distribution was used. This distribution was based on the selection among all available, only of *Tzz* or/and *Txx* points lying closest to the knots of a grid. In this way the distribution is more homogeneous and the selected data retain their initial positions along the GOCE orbit. The dimensions of the grid cell were depended on the latitude.

Ground test data (gravity anomaly) or gradients from the GGSS were selected in the same manner.

In all cases the input data were overlapping the prediction areas by one degree in latitude and 2-4 degrees in longitude.

The necessary covariance functions can be estimated either using *Tzz* data or free-air gravity anomalies, which both are isotropic.When gravity anomalies are not available, covariance functions only from *Tzz* data are to be estimated. The GRAVSOFT programs EMPCOV and COVFIT were used here.

In Figure 1 the empirical covariance function of *Tzz* at the orbit altitude in the Arctic polar cap is shown, estimated from *Tzz* observations included in the area bounded by ($80° < \varphi < 90°$, $-180° < \lambda < 180°$). In Figure 2, the corresponding model covariance function of free-air gravity anomalies on the surface of the Earth, computed from the empirical covariance function of *Tzz* is shown (line in red) together with the empirical covariance function of point free-air gravity anomalies in the same area (line in green) and the corresponding model covariance function of free-air gravity anomalies (line in blue). All data (*Tzz* and free-air) are reduced to EGM96 up to degree 36. All covariance functions have the same variance (about 750 $mGal^2$) and the same first zero-crossing point (about 2.5°) which fully agree to theory for degree 36.

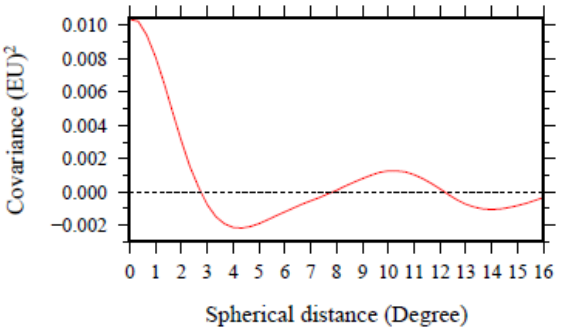

Figure 1. *Empirical covariance function of Tzz reduced to EGM96 up to degree 36, at GOCE orbit altitude.*

In the following tables the statistics of the results of the experiments in each test area are shown separately. The tables include the statistics of the collocation experiments using different parameters itemized in the previous section, the statistics of the reduction to EGMs SPW, TIM and DIR, as well as to TIM2 and DIR2. The bounds of each prediction area and the number of input data points as well as the number of the test point or mean data used are also included in these tables. A detailed discussion about the results of the various prediction experiments using the released GOCE observations and the reduction results using the GOCE EGM's is carried out in section 3.

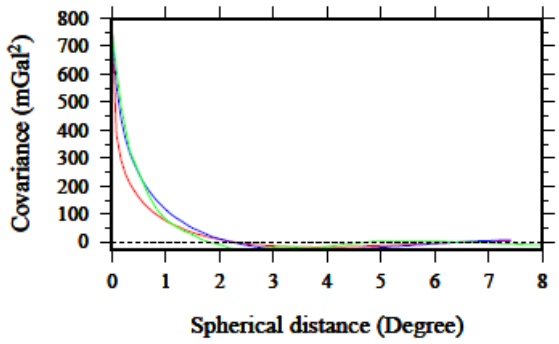

Figure 2*. Modeled covariance function of free-air gravity anomalies on the surface of the Earth (line in red) computed from the empirical covariance function of figure 1, empirical covariance function of point free-air gravity anomalies (line in green) and the corresponding modeled covariance function (line in blue).*

Oklahoma

A set of 9,608 free-air gravity anomaly data on a 4 km×4 km grid covering the area bounded by 33° < φ < 36°, -101° < λ < -96°, is available over Oklahoma. A set of 8,725 GOCE gradients covering the area 32° < φ < 37°, -105° < λ < -92° was used for the prediction of gravity anomalies. The covariance function used for the prediction experiments in Oklahoma was estimated using the available free-air gravity anomalies. The prediction was carried out using *Tzz* gradients and adopting common error equal to (a) 0.010 EU, (b) 0.015 EU, (c) 0.025 EU, (d) using *Tzz* and *Txx* gradients simultaneously, with a common error equal to 0.015 EU. Note that common error below 0.010 EU leads the system of normal equations in singularities. The results of these numerical experiments are shown in Table 1a. In the same table the results of the reduction of the test data to GOCE EGMs are included.

The statistics of the solutions (a), (b) and (c), carried out using different hypotheses for the accuracy of *Tzz* gradients, showed that the results are not sensitive for changes from 0.010 to 0.025 EU. The accuracy of 0.015 EU looks to be reasonable for the present status of the gradients. Furthermore, the combination of *Tzz* and *Txx* (solution d) yielded only a marginal improvement in the results.

A comparison of the prediction with the reduction results of Table 1 leads to hypothesis that the EGMs include more information than the observations, or that the observations include a noise which was removed during the development of the EGMs.

Table 1a*. Statistics of gravity anomalies over Oklahoma, predicted from GOCE Tzz or Tzz and Txx gradients, and reduced to GOCE EGMs. Unit is mGal.*

Oklahoma: 33° < φ < 36°, -101° < λ < -96°				
Data	Mean value	Standard deviation	Maximum	Minimum
Δg^{obs} (9,608)	-2.35	24.61	79.00	-62.00
Δg^{obs}- EGM96/36	9.33	24.78	92.29	-52.52
(a) Prediction using *Tzz* with error equal to 0.01 EU, number of available GOCE gradients 8,725				
Δg^{red} - Δg^{pred}	1.15	19.89	82.03	-49.30
(b) Prediction using *Tzz* with error equal to 0.015 EU, number of available GOCE gradients 8,725				
Δg^{red} - Δg^{pred}	1.24	19.87	80.94	-45.74
(c) Prediction using *Tzz* with error equal to 0.025 EU, number of available GOCE gradients 8,725				
Δg^{red} - Δg^{pred}	1.43	19.88	79.42	-45.04
(d) Prediction using *Tzz+Txx*, error equal to 0.015, number of available GOCE gradients 17,450				
Δg^{red} - Δg^{pred}	1.05	19.34	79.80	-47.11
Reduction to GOCE EGMs				
Δg^{obs}- SPW	1.07	17.96	73.05	-52.09
Δg^{obs}- TIM	1.41	17.80	73.06	-47.88
Δg^{obs}- DIR	1.21	16.07	67.89	-42.26
Δg^{obs}-TIM2	1.15	16.06	65.03	-46.20
Δg^{obs}-DIR2	0.75	16.51	66.90	-49.55

A comparison of the prediction with the reduction results of Table 1 leads to hypothesis that the EGMs include more information than the observations, or that the observations include a noise which was removed during the development of the EGMs. To test these hypothesis *Tzz* gradients were generated from DIR and new prediction experiments were carried out, using the same covariance function and a common error for the *Tzz* gradients equal to (e) 0.015 EU and (f) 0.02 EU. The statistics of these experiments are shown in Table 1b. In the first case (e) the standard deviation of the differences (observed – predicted) was reduced from 19.88 to 18.36 mGal. In the second case (f) the standard deviation dropped to 17.25 mGal, without having any singularity problem. The last two experiments endorse the hypothesis.

Table 1b. *Statistics of gravity anomalies over Oklahoma, predicted from Tzz generated from the DIR. Unit is mGal.*

Oklahoma: $33° < \varphi < 36°$, $-101° < \lambda < -96°$				
Data	Mean value	Standard deviation	Maximum	Minimum
Δg^{obs} (9,608)	-2.35	24.61	79.00	-62.00
Δg^{obs}- EGM96/36	9.33	24.78	92.29	-52.52
(e) Prediction using *Tzz* generated from DIR with error equal to 0.015, number of gradients 8,725				
Δg^{red} - Δg^{pred}	1.67	18.36	75.43	-45.33
(f) Prediction using *Tzz* generated from DIR with error equal to 0.002, number of gradients 8,725				
Δg^{red} - Δg^{pred}	1.37	17.25	70.72	-46.72
Reduction to GOCE EGMs				
Δg^{obs}- SPW	1.07	17.96	73.05	-52.09
Δg^{obs}- TIM	1.41	17.80	73.06	-47.88
Δg^{obs}- DIR	1.21	16.07	67.89	-42.26
Δg^{obs}-TIM2	1.15	16.06	65.03	-46.20
Δg^{obs}-DIR2	0.75	16.51	66.90	-49.55

Taiwan

Over Taiwan a number of 4,800 3'×3' grid free-air gravity values are available, within the bounds $21.5° < \varphi < 25.5°$, $119.5° < \lambda < 122.5°$. The number of observed gradients covering the wider area bounded by $20.5° < \varphi < 26.5°$, $115.5° < \lambda < 126.5°$ is 9,211. The variance of the gravity anomalies exceeds 4,918 $mGal^2$. The following prediction experiments were carried out in this very interesting test area: (a) prediction of gravity anomalies from *Tzz* gradients using a common error equal to 0.015 EU, (b) and (c) prediction of gravity anomalies from *Txx* using a common error equal to 0.025 and 0.075 EU, respectively, (d) prediction of gravity anomalies using *Tzz* and *Txx*. In all cases a covariance function estimated from the available gravity data was used. The results of these experiments are shown in Table 2a. It is remarkable that in an area with a very rough gravity field the results of the prediction using *Tzz* or *Tzz* and *Txx* gradients agreed very well with the results of the reduction, since in the much smoother test area of Oklahoma this was not shown. The prediction results using *Txx* gradients are very poor comparing to corresponding results using *Tzz* and the combination of *Tzz* with *Txx* failed to improve the prediction compared to when only *Tzz* gradients were used.

Finally the prediction of *Tzz* gradients at GOCE positions was attempted from the surface gravity anomalies. The covariance function estimated from the available gravity data was used. The statistics of this attempt is shown in Table 2b.

The standard deviation of the differences between GOCE *Tzz* observations and *Tzz* predicted from gravity equals to about 29% of the GOGE observations, while the standard deviation of the reduced GOCE *Tzz* to DIR up to degree 240 equals to about 14% of the GOCE observations. Taking into account that the corresponding results of the prediction of gravity from GOCE observations are

comparable, it might be concluded that a larger ground data-collection area and a higher order reference field is needed for upward continuation (see e.g. Arabelos and Tscherning, 1998).

***Table 2a**. Statistics of free-air gravity anomalies over Taiwan, predicted from GOCE Tzz or Txx or Tzz and Txx gradients, and reduced to GOCE EGMs. Unit is mGal.*

$20.5° < \varphi < 26.5°$, $115.5° < \lambda < 126.5°$, number of available gradients 9,211				
Data	Mean value	Standard deviation	Maximum	Minimum
Δg^{obs} (4,800)	15.25	70.13	339.39	-224.92
Δg^{red}- EGM96/36	11.51	70.34	336.36	-229.69
(a) Prediction using *Tzz* with error equal to 0.015 EU				
$\Delta g^{red} - \Delta g^{pred}$	-1.66	50.90	241.17	-193.64
(b) Prediction using *Txx* with error equal to 0.025 EU				
$\Delta g^{red} - \Delta g^{pred}$	2.85	60.29	277.94	-214.08
(c) Prediction using *Txx* with error equal to 0.075 EU				
$\Delta g^{red} - \Delta g^{pred}$	2.07	63.00	294.65	-218.51
(d) Prediction using *Tzz* with common error equal to 0.015 and *Txx* with error equal to 0.025				
$\Delta g^{red} - \Delta g^{pred}$	-1.37	50.75	238.94	-197.05
Reduction to GOCE EGMs				
Δg^{obs}- SPW	-0.93	51.88	229.94	-195.39
Δg^{obs}- TIM	-0.90	51.80	231.53	-196.78
Δg^{obs}- DIR	0.40	48.00	216.38	-181.55
Δg^{obs}- TIM2	-0.26	49.54	225.47	-186.38
Δg^{obs}- DIR2	0.10	48.10	230.15	-182.49

***Table 2b.** Statistics of the results of prediction of Tzz gradients at GOCE positions from ground gravity.*

$21.5° < \varphi < 25.5°$, $119.5° < \lambda < 122.5°$				
Tzz^{obs} (922)	0.1941	0.0982	0.3395	-0.0617
Tzz^{obs} -EGM96/36	0.0558	0.1555	0.3027	-0.3332
(e) prediction of *Tzz* at GOCE positions from mean 3'×3' free-air gravity anomalies (4,800)				
$Tzz^{red} - Tzz^{pred}$	-0.0116	0.0310	0.0550	-0.1234
Reduction of GOCE *Tzz* observations to GOCE EGMs				
Tzz^{obs} - SPW	0.0041	0.0169	0.0635	-0.0545
Tzz^{obs} - TIM	0.0031	0.0168	0.0621	-0.0552
Tzz^{obs} - DIR	0.0031	0.0167	0.0629	-0.0530
Tzz^{obs} - TIM2	0.0026	0.0169	0.0627	-0.0546
Tzz^{obs} – DIR2	0.0027	0.0168	0.0635	-0.0543

Mediterranean Sea

The gravity data covering the Mediterranean Sea are 5'×5' free-air gravity anomalies resulted by digitizing the free-air anomaly maps by Morelli. Based on previous experience with the behaviour of the gravity field in the Mediterranean the entire are was divided in three zones: western, central and eastern. Prediction experiments were conducted using all available GOCE observations over each of the three zones but also using observations with resolution of 8', in an attempt to estimate the effect of the density of the input data on the prediction results. The prediction of gravity anomalies was carried out using *Tzz* and combination of *Tzz* with *Txx* observations. Common error equal to 0.015EU was adopted for

these observations. The statistics of the computations are shown in Table 3.

Using all available *Tzz* observations the results in terms of the standard deviation observed – predicted are slightly better than corresponding results observations with resolution of 8'. For the same resolution, the combination of *Tzz* with *Txx* yielded slightly improved results than the use of *Tzz* observations only. However, these improvements could not be considered as significant.

Among the three zones, the prediction results in the (smoother) western zone are comparable with the results of the reduction of the gravity anomalies to GOCE EGMs. In the central and eastern test field differences appeared which are larger in the last (very rough) last one.

Table 3*. Statistics of free-air gravity anomalies over the Mediterranean Sea, predicted from GOCE Tzz or Txx or Tzz and Txx gradients, and reduced to GOCE EGMs. Unit is mGal.*

Mediterranean Sea: 31.0° < φ < 45.3°, -7.5° < λ < 37°				
Western Mediterranean: 31.0° < φ < 45.3°, -7.5° < λ < 14.0°				
Data	Mean value	Standard deviation	Maximum	Minimum
Δg^{obs} (8,383)	-1.89	24.93	84.09	-132.03
Δg^{obs}- EGM96/36	-15.76	25.29	74.02	-149.07
(a) Prediction using *Tzz* , common error 0.015 EU (all available 36,874)				
Δg^{red} - Δg^{pred}	-2.77	21.46	77.14	-97.74
(b) Prediction using *Tzz* , common error 0.015 EU (resolution 8', 10,821)				
Δg^{red} - Δg^{pred}	-2.72	21.58	76.79	-98.57
(c) Prediction using *Tzz* +*Txx* , common error 0.015 EU (resolution 8', 21,642)				
Δg^{red} - Δg^{pred}	-2.56	21.40	77.92	-99.51
Reduction to GOCE EGMs				
Δg^{obs}- SPW	-2.08	22.42	76.22	-103.22
Δg^{obs}- TIM	-1.58	21.44	70.41	-101.70
Δg^{obs}- DIR	-0.41	21.17	70.11	-91.01
Δg^{obs}- TIM2	-1.04	21.21	67.89	-97.18
Δg^{obs}- DIR2	-1.06	21.44	69.15	-94.04

Central Mediterranean: 30° < φ < 46.0°, 9.0° < λ < 27.0°				
Data	Mean value	Standard deviation	Maximum	Minimum
Δg^{obs} (4,027)	-9.27	50.86	119.82	-220.07
Δg^{obs}- EGM96/36	-9.02	46.24	133.63	-196.50
(a) Prediction using *Tzz* , common error 0.015 EU (all available 39,380)				
Δg^{red} - Δg^{pred}	-1.22	24.46	133.78	-129.48
(b) Prediction using *Tzz* , common error 0.015 EU (resolution 8', 10,929)				
Δg^{red} - Δg^{pred}	-1.58	24.88	113.28	-134.20
(c) Prediction using *Tzz* + *Txx* , common error 0.015 EU (resolution 8', 21,858)				
Δg^{red} - Δg^{pred}	-1.43	24.78	114.99	-135.46
Reduction to GOCE EGMs				
Δg^{obs}- SPW	-2.41	22.78	111.74	-116.01
Δg^{obs}- TIM	-2.29	22.28	113.81	-118.81
Δg^{obs}- DIR	-1.50	20.63	104.23	-113.05
Δg^{obs}- TIM2	-1.65	21.06	111.06	-116.63
Δg^{obs}- DIR2	-1.42	21.44	109.87	-122.30

Table 3 *continued*

Eastern Mediterranean: 31.2° < φ < 37.9°, 22.0° < λ < 39.5°				
Data	Mean value	Standard deviation	Maximum	Minimum
Δg^{obs} (3,162)	-50.23	52.04	118.75	-215.44
Δg^{obs}- EGM96/36	-41.06	50.80	103.49	-207.95
(a) Prediction using *Tzz* , common error 0.015 EU (all available 14,311)				
Δg^{red} - Δg^{pred}	-2.38	34.63	101.46	-153.34
(b) Prediction using *Tzz* + *Txx*, common error 0.015 EU (33,196)				
Δg^{red} - Δg^{pred}	-2.18	34.33	103.55	-146.14
(c) Prediction using *Tzz* + *Txx* , common error 0.015 EU (near 8' grid, 21,858)				
Δg^{red} - Δg^{pred}	-2.70	36.86	98.99	-154.87
Reduction to GOCE EGMs				
Δg^{obs}- SPW	-3.62	30.63	102.63	-123.26
Δg^{obs}- TIM	-2.79	28.64	102.89	-118.88
Δg^{obs}- DIR	-1.72	28.28	114.50	-141.47
Δg^{obs}- TIM2	-1.82	27.44	106.20	-135.96
Δg^{obs}- DIR2	-1.70	28.28	110.12	-136.12

Canadian plains

Point free-air gravity anomalies with a distribution about 2' are available over the Canadian plains, covering the area 56.0° < φ < 68.0°, -126.0° < λ < -106.0° (see Figure 3). The number of GOCE gradients into the wider area 54.0° < φ < 70.0°, -130.0° < λ < -102.0° is 63,113. Numerical experiments were carried out aiming at examine the effect of the density of the *Tzz* gradients on the prediction results. For this reason prediction were made with *Tzz* observations selected lying closest to the knots of a grid with cell dimension (a) 10', (b) 8' and (c) 5'. A covariance function estimated using all available gravity data was used and for the *Tzz* gradients a common error equal to 0.015 EU was adopted. All available (14,177) point gravity anomalies were used as test data set. The results are shown in Table 4.

Table 4*. Statistics of free-air gravity anomalies over the Canadian plains, predicted from GOCE Tzz gradients, and reduced to GOCE EGMs. Common error for Tzz equal to 0.015 EU was used. Gravity unit is mGal.*

Canadian Plains: 56.0° < φ < 68.0°, -126.0° < λ < -106.0°				
Data	Mean value	Standard deviation	Maximum	Minimum
Δg^{obs} (14,177)	-10.77	22.42	133.00	-81.10
Δg^{obs}- EGM96/36	0.34	22.28	122.28	-90.17
(a) Prediction using *Tzz* , resolution 10' (9,037)				
Δg^{red} - Δg^{pred}	0.65	18.23	122.97	-87.02
(b) Prediction using *Tzz* , resolution 8' (12,154)				
Δg^{red} - Δg^{pred}	0.54	17.37	128.03	-87.00
(c) Prediction using *Tzz* , resolution 5' (20,261)				
Δg^{red} - Δg^{pred}	0.18	17.43	122.12	-87.19
Reduction to GOCE EGMs				
Δg^{obs}- SPW	0.76	16.59	97.58	-106.53
Δg^{obs}- TIM	0.76	16.71	93.39	-108.11
Δg^{obs}- DIR	0.19	15.40	85.27	-114.93
Δg^{obs}- TIM2	-0.33	15.78	87.35	-117.54
Δg^{obs}- DIR2	-0.37	16.01	89.43	-119.08

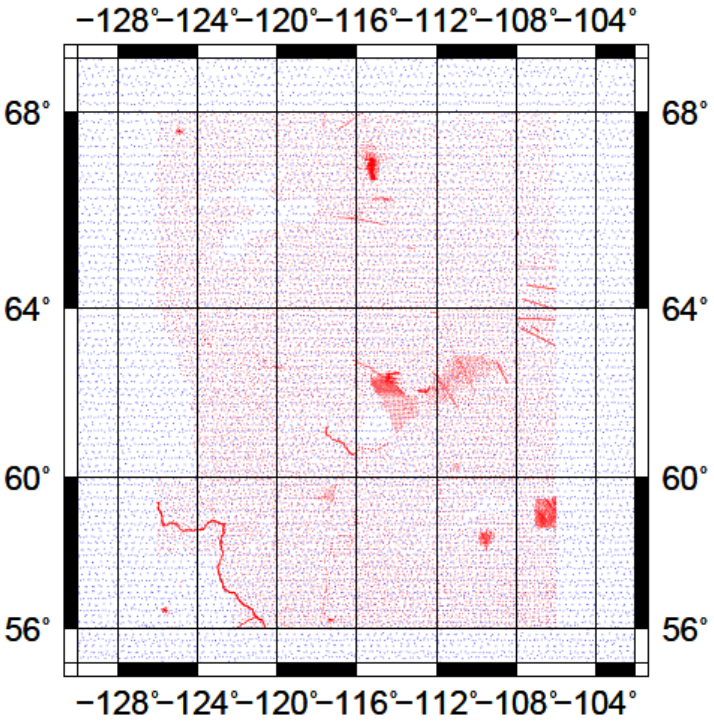

Figure 3. *GOCE observations over Canadian plains (blue dots) and gravity ground truth (red dots)*

Better prediction result in terms of standard deviation between Δg^{red} and predicted gravity anomalies yielded when a resolution equal to 8' was used for the input data, comparing to corresponding result with the thinner resolution of 10'. The denser resolution of 5' failed to improve further the standard deviation of 17.37 mGal, although the number of data points in the last case in considerably larger.

Scandinavia

The area bounded by $54.0° < \varphi < 64.0°$, $12.0° < \lambda < 30.0°$ is covered by 66,904 point free-air gravity anomalies consisting of terrestrial and airborne observations. The gravity field over Scandinavia is very smooth with a standard deviation equal to 18.6 mGal. GOCE *Tzz* and *Txx* observations covering the area $53.0° < \varphi < 65.0°$, $10.0° < \lambda < 32.0°$, with resolution 8' (see Figure 4), and common error equal to 0.015 EU were used for the prediction of gravity anomalies. The necessary covariance function was computed from all available (66,904) point free-air gravity anomalies. As in the previous test fields the combination of *Tzz* and *Txx* yielded slightly better results than the use of *Tzz* alone. The prediction results are very close to the reduction of the test gravity data to GOCE EGMs. The differences between observed free-air gravity anomalies and predicted values are shown in Fig. 3 and 4.

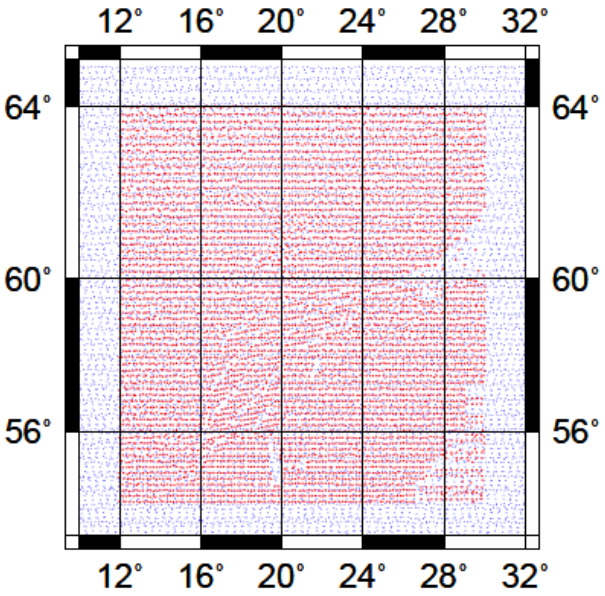

Figure 4. *GOCE observations over Scandinavia (blue dots) and gravity ground truth (red dots)*

Table 5. Statistics of free-air gravity anomalies over Scandinavia, predicted from GOCE *Tzz* or *Txx* or *Tzz* and *Txx* gradients, and reduced to GOCE EGMs. Unit is mGal.

Scandinavia: 54.0° < φ < 64.0°, 12.0° < λ < 30.0°				
Data	Mean value	Standard deviation	Maximum	Minimum
Δg^{obs} (6,306)	-10.75	19.72	64.44	-82.54
Δg^{obs}- EGM96/36	0.39	18.99	59.26	-74.49
(a) Prediction using *Tzz* (10,941) with resolution 8' and common error equal to 0.015 EU				
Δg^{red} - Δg^{pred}	-0.78	12.22	64.31	-50.37
(b) Prediction using *Tzz* and *Txx* (21,822) with resolution 8' and common error equal to 0.015 EU				
Δg^{red} - Δg^{pred}	-0.82	12.05	67.27	-51.20
Reduction to GOCE EGMs				
Δg^{obs}- SPW	-1.03	11.63	75.70	-47.76
Δg^{obs}- TIM	-1.12	11.97	73.16	-48.72
Δg^{obs}- DIR	-1.13	10.54	81.63	-46.29
Δg^{obs}- TIM2	-1.17	11.71	69.77	-46.15
Δg^{obs}- DIR2	-1.21	12.45	77.18	-49.98

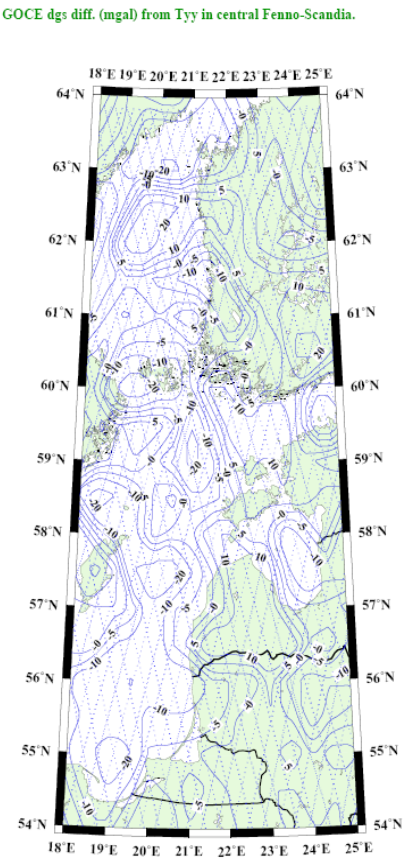

Fig 5.

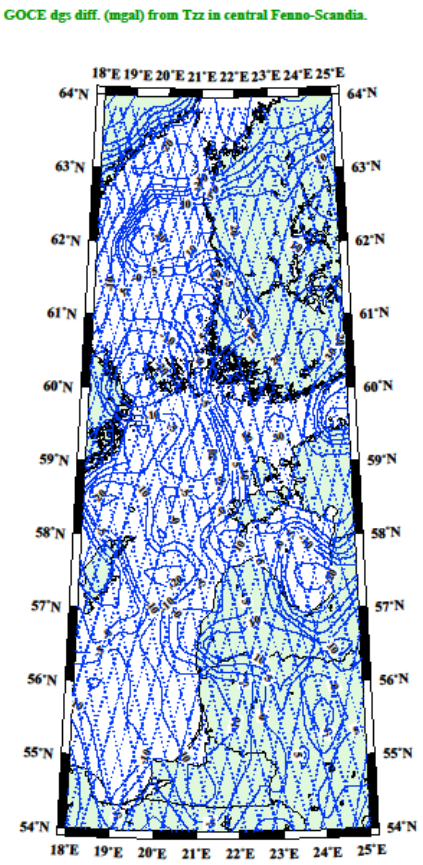

Fig. 6.

Australia

A data set consisting of 1,117,054 point free-air gravity anomalies is available for Australia, with a mean distance of about 0.5´. Due to this large amount of data the test area was divided in two parts, eastern and western. Observed *Tzz* gradients were used, lying closest to the knots of a 10'×10' grid. The prediction in the eastern part was carried out (a) using a "regional" covariance function estimated from free-air gravity anomalies with a resolution 10' covering both western and eastern part, and (b) using a "local" covariance function covering only the eastern part. The results are shown in Table 6. In the same table the results of the reduction of the test data to GOCE EGMs are included. Common error equal to 0.015 EU was adopted in all prediction experiments with Australian data. In Figure 7 the GOCE observations (blue dots) and the gravity ground truth (red dots) both with resolution 10' are shown.

The results of Table 6 show that the prediction does not depend on the covariance function, since the prediction results in the eastern Australian using the regional or the local covariance function are almost identical, although the covariances are different. The results of the reduction of the test data in the western part are considerably better tan those of the prediction. In the eastern part this is not valid, since both, prediction and reduction results does not differ substantially.

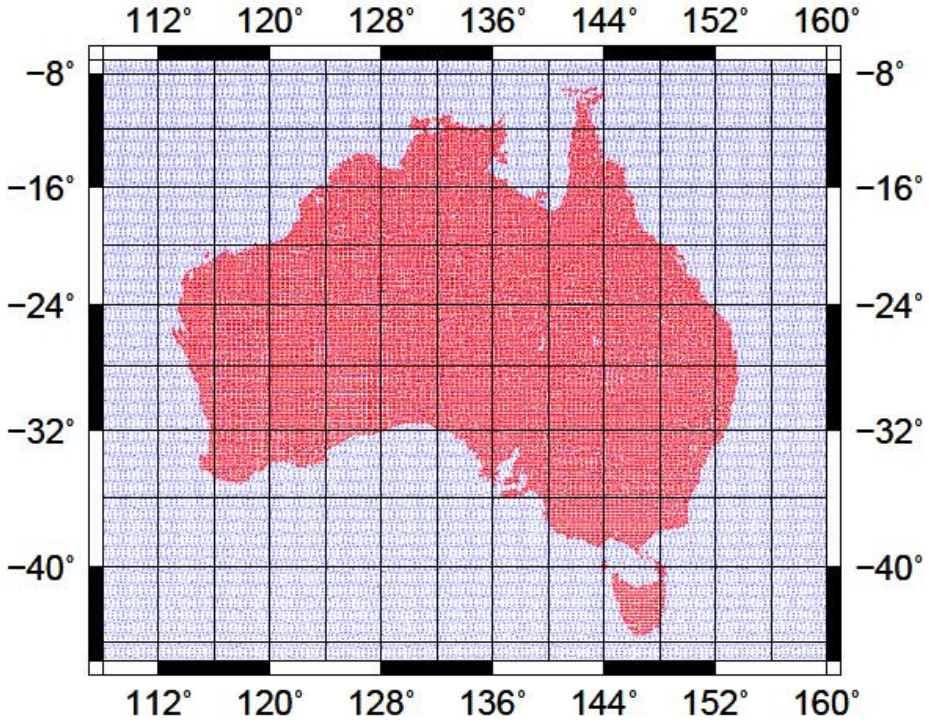

Figure 7. *GOCE observations over Australia (blue dots) and gravity ground truth (red dots)*

Table 6*. Statistics of gravity anomalies over Australia predicted from GOCE Tzz gradients, and reduced to GOCE EGMs. Unit is mGal.*

Australia: -42.8° < φ < -8°, -112.9° < λ < 153.6°				
Western part: -42.8° < φ < -8°, -110° < λ < 136°				
Data	Mean value	Standard deviation	Maximum	Minimum
Δg^{obs} (12,058)	-3.82	26.33	147.23	-211.33
Δg^{obs}-EGM96/36	0.34	23.97	166.97	-189.67
(a) Prediction using *Tzz*, regional covariance function, resolution 10'×10' (25,341)				
Δg^{red} - Δg^{pred}	-0.63	17.20	101.26	-199.41

Table 6 *continued*

Reduction to GOCE EGMs				
Δg^{obs}- SPW	-0.60	15.44	84.81	-191.74
Δg^{obs}- TIM	-0.63	14.75	85.18	-194.86
Δg^{obs}- DIR	-0.60	13.17	66.18	-198.28
Δg^{obs}- TIM2	-0.63	14.31	83.11	-206.27
Δg^{obs}- DIR2	-0.63	14.73	77.42	-204.81

Eastern Part: $-42.8° < \varphi < -8°$, $-110° < \lambda < 136°$				
Δg^{obs} (13,992)	10.82	21.73	145.87	-58.76
Δg^{obs}-EGM96/36	2.33	20.15	136.41	-58.57
(a) Prediction using *Tzz*, regional covariance function, resolution 10'×10' (23,336)				
Δg^{red} - Δg^{pred}	-0.98	14.18	109.22	-102.02
(b) Prediction using *Tzz*, local covariance function, resolution 10'×10' (23,336)				
Δg^{red} - Δg^{pred}	-0.98	14.17	109.40	-101.87
Reduction to GOCE EGMs				
Δg^{obs}- SPW	-1.12	14.03	101.04	-103.49
Δg^{obs}- TIM	-1.17	13.75	101.29	-98.12
Δg^{obs}- DIR	-1.11	12.77	109.39	-97.15
Δg^{obs}- TIM2	-1.14	13.74	105.95	-100.83
Δg^{obs}- DIR2	-1.17	14.54	109.86	-96.71

Arctic zone

For the area bounded by $64° < \varphi < 90°$, $-180° < \lambda < 180°$ a data set of 56,878 point free-air gravity anomalies is available, consisting of surface, marine and airborne observations. The number of the GOCE observations over the area $63° < \varphi < 90°$, $-180° < \lambda < 180°$ exceeds 1.2 millions. In order to facilitate the application of LSC the entire area was divided in three data collection zones A, B and C bounded by $64° < \varphi < 71°$, $-180° < \lambda < 180°$, $69° < \varphi < 81°$, $-180° < \lambda < 180°$ and $79° < \varphi < 90°$, $-180° < \lambda < 180°$ respectively and the prediction experiments were carried out using GOCE observations with resolution 20'×30' in the zones A and B, and 10'×30' in the zone C. *Tzz* observations were used in all zones and *Tzz* and *Txx* combination in zone C. Experiments using local or regional covariance functions were carried out in zones B and C. Common error equal to 0.015 EU was adopted for all prediction experiments. The results of these computations are shown in Table 7. The results using local or regional covariance functions in zones B and C are almost identical.

The combination of *Tzz* with *Txx* in the polar cap resulted in considerably lower prediction quality than the use of *Tzz* alone. The results of the prediction in zone C using *Tzz* alone are comparable to that of the reduction of the test data to GOCE EGMs.

Table 7*. Statistics of gravity anomalies over the Arctic Ocean predicted from GOCE Tzz or Tzz and Txx gradients, and reduced to GOCE EGMs. Unit is mGal.*

Arctic Ocean $64° < \varphi < 90°$, $-180° < \lambda < 180°$				
Zone A: $64° < \varphi < 70°$, $-180° < \lambda < 180°$, number of gradients 25,992, 20'×30' like grid				
Data	Mean value	Standard deviation	Maximum	Minimum
Δg^{obs} (21,469)	0.92	31.13	245.74	-127.14
Δg^{obs}-EGM96/36	-0.65	25.97	207.94	-155.30
Prediction using *Tzz* , local covariance function, resolution 20'×30', (17,159)				
Δg^{red} - Δg^{pred}	-0.47	20.23	191.53	-148.10

Table7 *continued*				
Reduction to GOCE EGMs				
Δg^{obs}- SPW	-0.66	19.17	187.51	-150.07
Δg^{obs}- TIM	-0.71	18.76	181.18	-142.05
Δg^{obs}- DIR	-0.75	17.86	183.11	-133.29
Δg^{obs}- TIM2	-0.75	18.63	188.56	-137.73
Δg^{obs}- DIR2	-0.76	18.87	190.52	-141.87

Zone B: 70° < φ < 80°, -180° < λ < 180°				
Δg^{obs} (10,514)	-0.51	29.20	179.84	-161.96
Δg^{obs}-EGM96/36	-1.67	26.19	167.32	-197.36
Prediction using *Tzz*, local covariance function, resolution 20'×30', (25,767)				
Δg^{red} - Δg^{pred}	-1.15	20.25	146.54	-199.65
Prediction using *Tzz*, regional covariance function , resolution 20'×30', (25,767)				
Δg^{red} - Δg^{pred}	-1.13	20.15	145.65	-201.93
Reduction to GOCE EGMs				
Δg^{obs}- SPW	-1.27	18.84	135.62	-204.76
Δg^{obs}- TIM	-1.24	18.57	122.06	-194.43
Δg^{obs}- DIR	-1.19	17.77	118.41	-184.28
Δg^{obs}- TIM2	-1.23	18.58	113.59	-181.13
Δg^{obs}- DIR2	-1.20	18.43	116.80	-182.64

Zone C: 80° < φ < 90°, -180° < λ < 180°				
Δg^{obs} (8,645)	5.51	28.35	162.40	-166.04
Δg^{obs}-EGM96/36	-1.57	27.48	157.24	-173.08
(a) Prediction using *Tzz* , local covariance function, resolution 10'×30', (19,048)				
Δg^{red} - Δg^{pred}	-1.74	21.73	121.33	-143.52
(b) Prediction using *Tzz* , regional covariance function, resolution 10'×30', (19,048)				
Δg^{red} - Δg^{pred}	-1.74	21.74	120.65	-143.52
(c) Prediction using *Tzz* + *Txx*, local covariance function, resolution 10'×30', (38,096)				
Δg^{red} - Δg^{pred}	-1.15	24.59	143.44	-141.98
Reduction to GOCE EGMs				
Δg^{obs}- SPW	-1.81	21.16	122.71	-120.79
Δg^{obs}- TIM	-1.87	22.42	116.08	-119.42
Δg^{obs}- DIR	-1.86	19.47	121.77	-124.49
Δg^{obs}- TIM2	-1.85	21.48	129.98	-121.02
Δg^{obs}- DIR2	-1.83	30.67	159.11	-148.34

The results using local or regional covariance functions in zones B and C are almost identical. The combination of *Tzz* with *Txx* in the polar cap resulted in considerably lower prediction quality than the use of *Tzz* alone. The results of the prediction in zone C using *Tzz* alone are comparable to that of the reduction of the test data to GOCE EGMs.

Antarctica

In Antarctica a set of 57,140 point free-air gravity anomalies are available from the Gravity Earth System data CD-ROM published by NOAA. The area covered by this data set is bounded by -90° < φ < -50°, -180° < λ < 180°. The number of GOCE observations into the area -90° < φ < -49°, -180° < λ < 180° exceeds 2 millions. For the same reasons discussed in the case of the Arctic Ocean, the entire area here was divided in four data collection zones, A, B. C and D with bounds -61° < φ < -49°, -180° < λ < 180°, -71° < φ < -59°, -180° < λ < 180°, -81° < φ < -69°, -180° < λ < 180° and -90° < φ < -79°, -180° < λ < 180°, respectively. Local covariance functions were used for the prediction of the test gravity data in each zone and a common error of the *Tzz* observations adopted equal to 0.015 EU. The resolution of the input data was 20'×30' for the zones A,B,C. For D experiments carried out using

resolutions 10' × 60' and 10' × 20'. Due to some obviously erroneous extremely large values located in zone B the prediction in this zone was carried out using *Tzz* generated from GOCE EGM DIR. This is the reason of the more or less agreement of the prediction with the reductions to GOCE EGMs in this zone. This result is endorsing the discussion related to the similar experiment in Oklahoma. The results of these experiments are shown in Table 8.

The prediction results of the zone D (south polar cap) are comparable with the reduction results to GOCE EGMs. The prediction results using the higher resolution of 10'×20' with threefold number of *Tzz* observations than the lower resolution of 10'×60' were left almost unchanged.

In zones A and C the results of the reduction to EGMs are better than the corresponding prediction results.

Table 8*. Statistics of gravity anomalies over the Antarctica predicted from GOCE Tzz gradients, and reduced to GOCE EGMs. Unit is mGal.*

Antarctica: $-90° < \varphi < -50°$, $-180° < \lambda < 180°$				
Zone A: $-60° < \varphi < -50°$, $-180° < \lambda < 180°$				
Data	Mean value	Standard deviation	Maximum	Minimum
Δg^{obs} (19490)	7.40	33.44	254.50	-183.50
Δg^{obs}-EGM96/36	5.63	32.09	260.59	-181.74
Prediction using *Tzz* , local covariance function, resolution 20'×30', (25,992)				
Δg^{red} - Δg^{pred}	5.49	27.95	248.51	-169.17
Reduction to GOCE EGMs				
Δg^{obs}- SPW	4.74	25.21	236.12	-142.51
Δg^{obs}- TIM	4.42	24.81	229.29	-141.14
Δg^{obs}- DIR	4.68	22.83	222.34	-126.18
Δg^{obs}- TIM2	4.79	24.03	237.18	-136.27
Δg^{obs}- DIR2	4.41	24.65	234.63	-139.67
Zone B: : $-70° < \varphi < -60°$, $-180° < \lambda < 180°$				
Δg^{obs} (10,286)	7.35	35.21	250.60	-157.00
Δg^{obs}-EGM96/36	8.20	31.39	246.19	-176.61
Prediction using *Tzz* generated from DIR , local covariance function , resolution 20'×30', (25,814)				
Δg^{red} - Δg^{pred}	8.11	26.48	276.98	-173.49
Reduction to GOCE EGMs				
Δg^{obs}- SPW	6.46	25.94	271.01	147.50
Δg^{obs}- TIM	6.73	25.67	275.55	-147.38
Δg^{obs}- DIR	7.14	24.75	276.80	-141.11
Δg^{obs}- TIM2	6.66	25.63	269.67	-137.13
Δg^{obs}- DIR2	6.36	26.54	275.09	-137.59
Zone C: $-80° < \varphi < -70°$, $-180° < \lambda < 180°$,				
Δg^{obs} (5,508)	-8.56	44.88	176.30	-377.80
Δg^{obs}-EGM96/36	3.70	37.91	156.20	-350.18
Prediction using *Tzz* , local covariance function , resolution 20' × 30' , (25,970)				
Δg^{red} - Δg^{pred}	1.75	36.93	349.51	-351.95
Reduction to GOCE EGMs				
Δg^{obs}- SPW	0.23	32.93	145.82	363.55
Δg^{obs}- TIM	0.08	31.96	142.15	-369.62
Δg^{obs}- DIR	0.56	32.41	147.49	-356.96
Δg^{obs}- TIM2	0.23	31.78	132.97	-364.33
Δg^{obs}- DIR2	0.02	32.14	139.54	-354.85

***Table 8**.continued*

Zone D: -90° < φ < -80°, -180° < λ < 180°,				
Δg^{obs} (1,929)	-13.64	34.28	142.60	-167.60
Δg^{obs}-EGM96/36	-2.87	32.29	155.35	-142.26
Prediction using *Tzz* , loca covariance function, resolution 10' × 60' (9,518)				
Δg^{red} - Δg^{pred}	-0.73	28.77	138.95	-138.33
Prediction using *Tzz* , local covariance function, resolution 10' × 20' (28,506)				
Δg^{red} - Δg^{pred}	-0.41	28.48	136.18	-144.28
Reduction to GOCE EGMs				
Δg^{obs}- SPW	-0.94	27.07	147.74	-146.71
Δg^{obs}- TIM	3.92	29.36	149.20	-148.30
Δg^{obs}- DIR	-1.13	26.52	148.05	-153.00
Δg^{obs}- TIM2	4.57	29.24	155.67	-144.46
Δg^{obs}- DIR2	-1.25	32.44	155.96	-147.91

Prediction of GGSS Tzz from GOCE Tzz over Oklahoma

The prediction of *Tzz* data from GGSS at a height of 1000 m over Oklahoma was attempted, using *Tzz* gradients from GOCE. From the available 45,219 GGSS *Tzz* data points 5,616 were selected, lying closest to the knots of a 0.05' grid. The results of this experiment are shown in Table 9. The statistics show that both, the prediction and the reduction to GOCE EGMs failed to change the original figure of the GGSS data, probably due to their poor quality.

***Table 9**. Statistics of GGSS Tzz over Oklahoma, predicted from GOCE Tzz, and reduced to GOCE EGMs. Unit is EU.*

33° < φ < 36°, -101° < λ < -96°, number of available GOCE gradients 8,725 (near 0.5' grid)				
Data	Mean value	Standard deviation	Maximum	Minimum
Tzz^{obs} (5,616)	-8.76	23.51	81.72	-112.29
Tzz^{obs}-EGM96/36	-8.13	23.52	82.43	-111.73
(a) Prediction using GOCE *Tzz* with error equal to 0.015 EU				
Tzz^{red} - Tzz^{pred}	-10.16	23.26	82.02	-116.62
Reduction to GOCE EGMs				
Tzz^{obs} - SPW	-10.21	23.19	78.79	-117.41
Tzz^{obs} - TIM	-9.90	23.22	80.38	-116.96
Tzz^{obs} - DIR	-9.67	23.12	78.68	-115.97
Tzz^{obs} - TIM2	-9.69	23.14	79.34	-117.78
Tzz^{obs} - DIR2	-9.77	23.29	80.20	-116.36

3. DISCUSSION

From the experiments carried out the following conclusions might be drawn related to the investigated parameters:

- *Tzz* include the major part of information comparing to *Txx*. This is clear in the case of prediction of gravity using separately *Tzz* or *Txx* observations over Taiwan. This conclusion is supported from all experiments using combination of *Tzz* and *Txx* for the prediction of gravity anomalies over Oklahoma, Taiwan, Mediterranean Sea, and Scandinavia and over a part of the Arctic Ocean: The improvement in the prediction results due to the additional use of *Txx* is in all these cases marginal. This conclusion

agrees with corresponding conclusions deduced from simulation studies.

- The hypothesis of the accuracy of the GOCE observations plays a role in the prediction. Small changes of the common error adopted for *Tzz* data (e.g. from 0.010 to 0.025 EU) caused small changes of the prediction results over Oklahoma, while larger changes of the common error adopted for *Txx* data (e.g. from 0.025 to 0.075 EU) resulted in significant changes of the prediction results over Taiwan. Smaller error than 0.01 EU leads the system of linear equation in singularities (due to the low degree reference field subtracted). When data generated from the GOCE EGMs are used (e.g. DIR) much smaller (down to 0.002 EU) common error can be used without the problem of singularities, yielding better prediction results as it is shown in two relevant experiments over Oklahoma.

- The distribution of the GOCE observations plays also a role in the prediction. It could not be concluded from experiments over Oklahoma and Taiwan, where all available GOCE observations are used, but from the experiments in all other test areas where either all available observations or/and part of them are used. In Western and Central Mediterranean Sea, where test data are mean 5'×5' gravity anomalies the use of all available GOCE *Tzz* observations yielded slightly better results than a distribution with a resolution of 8'. However, we are not trying to correlate the distribution of the observations with the distribution of the test data. Over Canadian plains prediction experiments were conducted using observations with resolutions of 10', 8' and 5'. In this case, the prediction results were better when the resolution of the data was 8'. Note that the distribution of GOCE data over Canadian plains is denser than over Mediterranean, due to the latitude difference. Generally speaking, dense distribution of the input data yields better prediction results. The problems with the dense distribution in the Canadian plain would have been solved, if we had subtracted a reference field of higher degree, and consequently obtained a covariance function with shorter correlation distance, thereby de-correlating the data.

- The dependence of the prediction results on the covariance function was examined over Australia, and the Arctic Ocean. In the experiments carried out in parts of these extended areas "local" or "regional" covariance functions were used, i.e. covariance functions estimated from the gravity data lying in each individual part, or in the corresponding entire test area. All other parameters were kept same. In Eastern Australia the difference in the prediction results using local or regional covariance function is negligible, while over Arctic Ocean the differences are marginal. These results suggest that the covariance function does not affect the prediction, at least so much as we had concluded in corresponding simulation studies. The fact that we have only subtracted low frequencies of the gravity spectrum might be the reason.

- In Table 10 the test fields used in this investigation are classified according to the standard deviation of their gravity anomalies. In the last column the difference *d* between the standard deviation of the observations std_o and of the difference (observation – predictions) std_p according to

$$d = \sqrt{std_o^{\,2} - std_p^{\,2}}\,,$$

is shown for the corresponding test field.

Table 10. *Classification of the test areas based on the standard deviation of the included gravity observation and the corresponding differences between the standard deviation of the observations and the standard deviation (observed – predicted) gravity anomalies. Unit is mGal.*

Test area	std_o	d
Scandinavia	19.7	14.7
Australia East	21.7	14.3
Canadian plains	22.4	14.0
Australia West	26.3	16.7
Oklahoma	24.6	15.5
Mediterranean Western	24.9	13.5
Arctic Ocean, zone C	28.4	16.8
Arctic Ocean, zone B	29.2	16.7
Arctic Ocean, zone C	31.1	16.3
Antarctica, zone A	34.4	15.8
Antarctica, zone D	34.3	14.7
Antarctica, zone B	35.2	16.9
Antarctica, zone C	44.9	25.5
Mediterranean Central	50.9	39.0
Mediterranean Eastern	52.0	37.0
Taiwan	70.1	48.7

From Table 10 it is shown that generally, in areas with very rough gravity field (such as Taiwan, Central and Eastern Mediterranean) the standard deviation of the predicted gravity anomalies dropped down much more than it happened in

areas with smooth gravity field. From this point of view we can consider the prediction more "successful" in areas with a rough than in a smooth gravity field.

The results of the reduction of gravity anomalies to GOCE EGMs of release 1 are in most cases better or slightly better than the results of the prediction using the GOCE gradient observations. This fact led to the hypothesis that EGMs include some more information comparing to the gradient observations, or some noise included in the gradients was filtered during the development of the EGMs. The hypothesis was endorsed from the results of prediction of gravity from *Tzz* gradients extracted from DIR, over Oklahoma. Among the three models the reduction to DIR resulted in better statistics over TIM and even better compared to SPW. One of the reasons is probably the extended degree of expansion of DIR, over SPW and TIM. The situation is different in the case of the EGMs TIM and DIR of release 2. TIM2 resulted in better statistics over TIM in all test areas except of the Arctic zone B (reduction of gravity anomalies) and Taiwan (reduction of *Tzz* observations, see Table 2b). This could be due to the increased degree of expansion of TIM2 from 224 to 250. On the other hand, DIR remains superior to DIR2 in all test areas except of Central and Eastern Mediterranean and Antarctica, zone C. The improvement of TIM2 over TIM is mostly not significant in spite of the increased degree of expansion. The problem with DIR2 is very serious in both polar caps.

ACKNOWLEDGMENT

This paper is prepared to the 4th GOCE user workshop, München, March 31 – April 1, 2011.

REFERENCES

Arabelos, D. & C.C.Tscherning: Calibration of satellite gradiometer data aided by ground gravity data. Journal of Geodesy, Vol. 12, no. 11, pp. 617 - 625, 1998.

Arabelos DN, Tscherning CC: A comparison of recent Earth gravitational models with emphasis on their contribution in refining the gravity and geoid at continental or regional scale J Geod 84:643-660. DOI 10.1007/s00190-010-0397-z, 2010.

Forsberg, R. and C.C.Tscherning: An overview manual for the GRAVSOFT Geodetic Gravity Field Modelling Programs. 2.edition. Contract report for JUPEM, 2008.

Förste, Ch., Flechtner, F., Schmidt, R., K¨onig, R., Meyer U., Stubenvoll R., Rothacher M., Barthelmes F., Neumayer, H., Biancale, R., Bruinsma, S., Lemoine, J. M. and Loyer, L.: A mean global gravity field model from the combination of satellite mission and altimetry/gravimetry surface data -EIGEN-Gl04C, Geophysical Research Abstracts, 8, 03462, 2006.

HPF: GOCE Level 2 Product Data Handbook, GO-MA-HPF-GS-0110, C Issue 4.3, 09.12.2010.

Lemoine, F.G., S.C. Kenyon, J.K. Factor, R.G. Trimmer, N.K. Pavlis, D.S. Chinn, C.M. Cox, S.M. Klosko, S.B. Luthcke, M.H. Torrence, Y.M. Wang, R.G. Williamson, E.C. Pavlis, R.H. Rapp, and T.R. Olson, The Development of the Joint NASA GSFC and the National Imagery and Mapping Agency (NIMA) Geopotential Model EGM96, NASA/TP-1998-206861, Goddard Space Flight Center, Greenbelt, MD, July, 1998.

Pavlis, N.K., S.A. Holmes, S.C. Kenyon, and J.K. Factor, An Earth Gravitational Model to Degree 2160: EGM2008, presented at the 2008 General Assembly of the European Geosciences Union, Vienna, Austria, April 13-18, 2008.

Tscherning, C.C.: A FORTRAN IV Program for the Determination of the Anomalous Potential Using Stepwise Least Squares Collocation. Reports of the Department of Geodetic Science No. 212, The Ohio State University, Columbus, Ohio, 1974.